DOI: 10.1007/s12541-010-0024-1

Sensitivity Control of a MR-Damper Semi-Active Suspension

Arjon Turnip[1], Seonghun Park[1] and Keum-Shik Hong[2,#]

1 School of Mechanical Engineering, Pusan National University, Jangjeon-dong, Geumjeong-gu, Busan, Korea, 609-735
2 Department of Cogno-Mechatronics Engineering, Pusan National University, Jangjeon-dong, Geumjeong-gu, Busan, Korea, 609-735
Corresponding Author / E-mail: kshong@pusan.ac.kr, TEL: +82-51-510-2454, Fax: +82-51-514-0685

KEYWORDS: Semi-active suspension, MR damper, Sensitivity control, Gradient algorithm, Polynomial model, Ride comfort

In this paper, numerical aspects of a sensitivity control for the semi-active suspension system with a magneto-rheological (MR) damper are investigated. A 2-dof quarter-car model together with a 6th order polynomial model for the MR damper are considered. For the purpose of suppressing the vertical acceleration of the sprung-mass, the square of the vertical acceleration is defined as a cost function and the current input to the MR damper is adjusted in the fashion that the current is updated in the negative gradient of the cost function. Also, for improving the ride comfort, a weighted absolute velocity of the sprung-mass is added to the control law. The implementation of the proposed algorithm requires only the measurement of the relative displacement of the suspension deflection. The local stability of the equilibrium point of the closed loop nonlinear system is proved by investigating the eigenvalues of the linearized one. Through simulations, the passive suspension, the skyhook control, and the proposed sensitivity control are compared.

Manuscript received: February 28, 2008 / November 26, 2009

1. Introduction

Magneto-rheological (MR) fluids have recently become a widely studied smart fluid and being widely used in industrial applications (such as car suspension, seat suspension, bridge vibration control, washing machine vibration control, and gun vibration control) since it require only small voltages and currents compared to other classes of fluids that exhibit a rheological change. This paper focuses on a sensitivity control (a type of gradient approach) in a car suspension system, which can adjust the current input to the MR damper.[1-10] However the concept presented herein can be extended to other applications.

The performance of a suspension systems can be evaluated by three criteria. These are the ride quality, which is related to the suppression of road disturbances; the handling performance of a vehicle, which is achieved by maintaining the traction force between the tire and the road surface; and the cost of the suspension system, which is related to the control force mechanism. According to the mechanism that produces the damping/control forces, suspension systems are classified into passive, semi-active, and active systems. A passive suspension consists of an energy dissipating element, which is a damper with a fixed-size orifice, and an energy-storing element, which is a spring stiffness for sustaining the vehicle weight. These two elements of passive suspension can not add energy to the system (such as the damping force generated from a fixed-size orifice is dependent only on the relative velocity of the suspension system), therefore it can not provide sufficient control force to improve the ride quality and handling performance for various road disturbances.

Due to the fact that a passive suspension cannot satisfy the comfort and handling requirement in different road conditions, a great deal of interest is being devoted to the control of semi-active and active suspension systems by both academia and industry.[11-52] To improve the ride quality, it is important to isolate the sprung-mass (the car body) from the road disturbances and, particularly, to suppress the vertical vibrations near 5 Hz (4-8 Hz), which is a sensitive frequency range to the human body (and the lateral vibrations at 1-2 Hz) according to ISO 2631.[19,20] On the other hand, to improve the handling performance of the vehicle, it is important to keep the tire in contact with the road surface so that the engine torque can be transmitted, as a traction force, to the road surface. Different kinds of control strategies have been proposed, which are more or less effective and attractive from a commercial point of view. Particularly in the control of active suspension systems, interesting results have been presented by Alleyne and Hedrick[32] where a modified adaptation scheme based on Lyapunov analysis is

used to provide solutions for the problems at hand.

Since a semi-active suspension system was introduced in the early 1970s, it has shown a comparable performance with that of a fully active suspension but with lower energy consumption. However, the fully active suspension system produces the control force with a separate hydraulic/pneumatic unit. Therefore, the cost and the weight of a fully active suspension system are disadvantageous in medium size cars. The semi-active suspension system uses a varying damping force as the control force. For example, a hydraulic continuous-damping-control (CDC) damper varies the size of an orifice in the hydraulic flow valve to generate the desired damping forces. On the other hand, a MR damper applies various levels of magnetic fields to vary the viscosities of the MR fluids.[3-7,40-43] However, the semi-active suspension system shows worse performance than the active system because the control force can be generated only when the desired control force and the damping force act in the same direction. From this view, semi-active suspension systems are better than the fully active systems because of their low cost and competitive performance.

For a fixed suspension spring stiffness coefficient, a better isolation of the sprung-mass from the road disturbances can be achieved with the use of a soft damping that allows a larger suspension deflection. However, a better road contact can also be achieved with the use of a hard damping that avoids unnecessary suspension deflections. These requirements are mutually conflicting in the control system design of suspension systems. To meet these requirements, many kinds of semi-active suspension are currently being employed and studied.

Since the skyhook control strategy was introduced by Karnopp et al.,[9] in which a fictitious (skyhook) damper is assumed between the sprung-mass and the stationary sky as a way to suppress the vibratory motions of the sprung-mass and as a tool to compute the desired damping force, a number of innovative control methodologies have been introduced in the literature. The skyhook configuration[5,7,17,32] isolates the sprung-mass from base excitations, at the expense of an increased unsprung-mass motion. Notice that as the skyhook damping ratio increases, the resonant transmissibility near 1 Hz decreases, but the transmissibility near 11 Hz increases. In essence, the skyhook configuration is adding more damping to the sprung-mass and taking away damping from the unsprung-mass. Hence, the skyhook damper alone cannot reduce both resonant peaks at the same time. For this reason, Besinger et al.[49] proposed a modification of the skyhook control, which includes both a passive damper as well as a skyhook damper, for the computation of desired control inputs. Novak and Valasek[50] have proposed the groundhook control, which assumes an additional fictitious damper between the unsprung-mass and the ground, to decrease the dynamic tire force.

Moreover, the implementation of the skyhook control needs two pieces of information: the absolute velocity of the sprung-mass and the relative velocity between the sprung and unsprung masses. In this paper, the measurement of only the suspension relative displacement between the sprung and unsprung masses and the use of a MR damper are assumed. The damping force of the MR damper is modeled as a 6th order polynomial equation of the relative velocity with coefficients as affine functions of the input current. The current input to the MR damper is adjusted, in principle, in the negative direction of the gradient vector of the square of the vertical acceleration of the sprung-mass, but considering the handling performance, a weighted absolute value of the sprung-mass velocity has been added in the law. The stability of the proposed nonlinear control law has been analyzed at equilibrium points.

In this paper, first, a new polynomial model for MR dampers that utilizes the peak damping forces due to sinusoidal velocity inputs is proposed. Second, with the use of only the relative displacement between the sprung and unsprung masses, a control algorithm that adjusts the current input to the MR damper such that the square of the vertical vibration is minimized is proposed and its stability is proved. Third, for balancing the ride quality and the handling performance, two adjustable parameters are incorporated in the control law.

This paper has the following structure. In Section 2, a quarter-car model and a new model for MR dampers are introduced. In Section 3, a modified gradient algorithm for adjusting the current input to the MR damper that minimizes the square of the vertical acceleration is proposed. In Section 4, the stability of the closed loop system at equilibrium points is proved. In Section 5, the performances of a passive system, a skyhook control system, and the system with the proposed modified gradient algorithm are compared by simulations. Section 6 presents the conclusions.

2. Quarter Car and MR Damper

2.1 A Quarter-Car Model

In semi-active suspensions, while the conventional suspension-spring configuration is kept, the damper with a fixed orifice is replaced with a controllable one. Fig. 1 depicts a control block diagram of the semi-active suspension system, where z_s, z_u, and z_r are the sprung-mass, the unsprung-mass, and the road displacements, respectively. The values of the parameters in this model are collected in Table 1. Based on the measurement of the relative displacement $z_s - z_u$, the control strategy is to adjust the damping force f_{mr} by applying the desired current input I to the MR damper. The estimation and modified sensitivity control will be discussed in Section 3.1 and Section 3.2, respectively. In addition to the intrinsic vertical motions limited to this quarter model, other

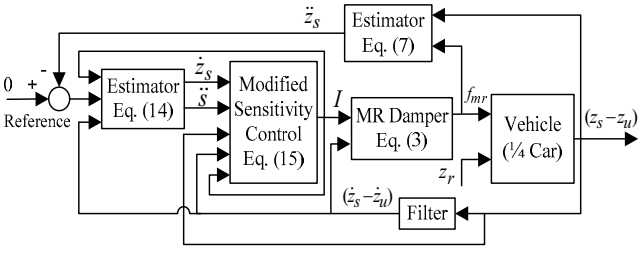

Fig. 1 Control block diagram of the semi-active suspension system

issues such as the pitch and roll controls of the vehicle are not discussed in this paper. The equations of motion are as follows,

$$m_s\ddot{z}_s + k_s(z_s - z_u) + f_{mr}(\dot{z}_s - \dot{z}_u, I) = 0, \quad (1)$$

$$m_u\ddot{z}_u + k_t(z_u - z_r) - k_s(z_s - z_u) - f_{mr}(\dot{z}_s - \dot{z}_u, I) = 0, \quad (2)$$

where f_{mr} is a function of the relative velocity $\dot{z}_s - \dot{z}_u$ and the current input I. Note that only the relative displacement $z_s - z_u$ is measured.

Table 1 Parameter values used in simulation

Parameters	definitions	values
m_s	Sprung-mass	390 kg
m_u	Unsprung-mass	41 kg
k_s	Spring stiffness coefficient	25,000 N/m
k_t	Tire stiffness coefficient	170,000 N/m

2.1.1 MR Damper Modeling

The semi-active dampers include the hydraulic discrete damping control damper using a step motor, the hydraulic continuous variable damper (CVD) using a solenoid valve, the ER damper, and the MR damper. Since the fluid used in an ER or MR damper has a fast response time, it can be used to cope with a broader range of road conditions. Also, the MR damper is the most suitable for car applications since the strength of an MR fluid is 20-50 times higher than that of an ER damper and less performance degradation due to impurities and precipitation has been reported. One notable feature of MR fluids is the hysteresis characteristics appearing in the expansion and contraction processes. Among the various models available in the literature, the model of Bingham[53] is the simplest model, but it may not fully characterize the hysteresis behavior; the model of Bouc-Wen[54-56] needs a very small step size when solving a steep differential equation numerically; and the nonparametric model of Song et al.[4] might be another potential candidate.

In this paper, an algebraic approach rather than a differential equation approach is pursued. Fig. 2 shows three hysteresis curves

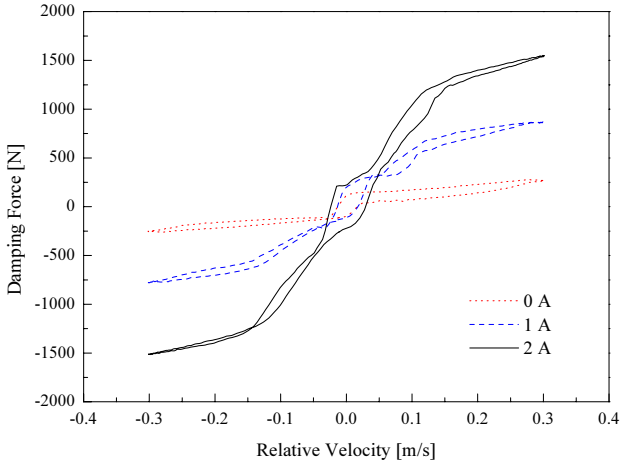

Fig. 2 Hysteresis curves of the used MR damper when $\dot{z}_s - \dot{z}_u = 0.3\cos 7.5t$ [11]

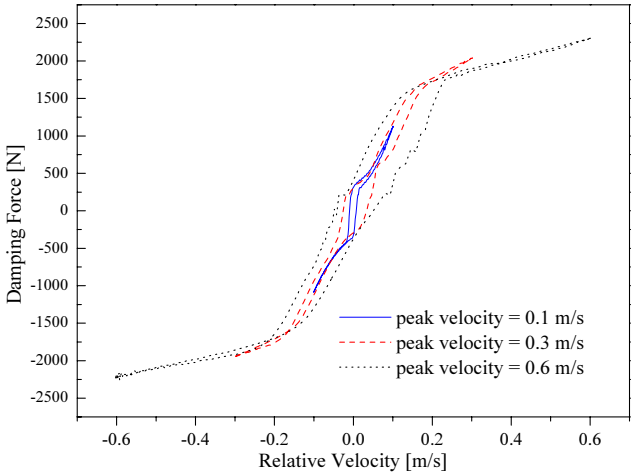

Fig. 3 Hysteresis curves for three sinusoidal relative displacements with 3 A current input[11] ($z_s - z_u = 0.04\sin 2.5t$, $0.04\sin 7.5t$, $0.04\sin 15t$, and $I = 3A$)

for three current inputs, respectively, for a typical MR damper, when $\dot{z}_s - \dot{z}_u = 0.3\cos 7.5t$ (*i.e.*, $z_s - z_u = 0.04\sin 7.5t$). The damping force increases as the relative velocity increases. Also, the slope gets steeper as the current input increases. However, for a fixed current input, the damping forces follow different curves in the expansion (the lower curve) and contraction (the upper curve) regions; this behavior is known as the hysteresis effect.

On the other hand, for a fixed current input at 3 A, Fig. 3 shows three different hysteresis curves of three different sinusoidal relative-displacement profiles with the same magnitudes but different frequencies, that is, $z_s - z_u$ = 0.04 sin 2.5*t*, 0.04 sin 7.5*t*, and 0.04 sin 15*t*. By differentiating them, $\dot{z}_s - \dot{z}_u = 0.1\cos 2.5t$, $0.3\cos 7.5t$ and $0.6\cos 15t$ are obtained, which correspond to three peak velocities 0.1, 0.3, and 0.6 m/s, respectively. The strategy in this paper is to consider the peak damping forces at individual peak-velocity points (instead of considering two hysteric curves in the expansion and contraction regions). In this case, one polynomial equation for a given current input (representing the peak damping forces) will be sufficient in representing the damping force characteristics as follows:

$$f_{mr}(\dot{z}_s - \dot{z}_u, I) = \sum_{k=0}^{n}(a_k^{\circ} + b_k^{\circ} I)(\dot{z}_s - \dot{z}_u)^k, \quad n = 6 \quad (3)$$

where n is the order of the polynomial (n =6 is used in this paper) and a_k^0 and b_k^0 are the coefficients that should be determined through experiments. Fig. 4 shows the characteristics of the actual nonlinear force-velocity of MR damper used in this work (seven of such curves correspond to seven different current inputs, and the lowest slope represents the passive system with zero current input). Table 2 shows a typical combination of the coefficients obtained from experiments for a SM_FRONT_Left MR CDC damper of Daewoo Precision Industries, Ltd., Korea. Fig. 5 depicts the experimental test bed using an MTS system. The closeness between experimental data and the values calculated from the polynomial model of (3) for three different current inputs (0, 1, and 2 A) is well depicted in Fig. 5 of reference 11.

Table 2 Coefficients a_k° and b_k° in (3) obtained from experimental data using the peak values[11]

Coefficients	Values	Coefficients	Values
a_0°	0	b_0°	11.6
a_1°	989.1	b_1°	1228.5
a_2°	17.4	b_2°	-56
a_3°	-316.3	b_3°	-970.5
a_4°	19	b_4°	52.2
a_5°	98.1	b_5°	254.3
a_6°	1.1	b_6°	-16.9

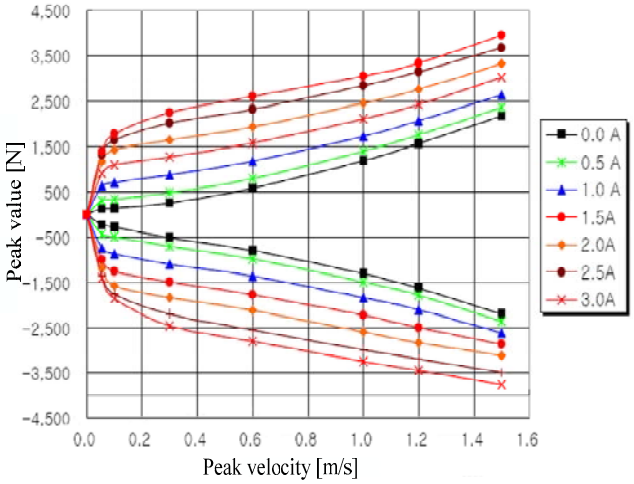

Fig. 4 Peak values of a typical MR CDC damper for various current inputs

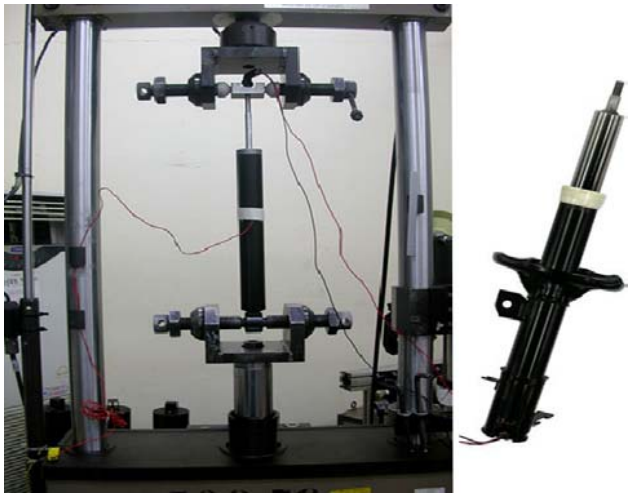

Fig. 5 Damping force measurement with an MTS System

3. Sensitivity Control

3.1 Control Law

In this paper, the measurement of the relative displacement is assumed. The square of the vertical acceleration is considered as a performance criterion to be minimized as follows.

$$J = \ddot{z}_s^2. \tag{4}$$

In (1), $\ddot{z}_s$ is a function of I (of course, it is also a function of other variables and parameters). For computing the current input, the following control law is proposed.

$$\dot{I} = -\mu_1 \frac{\partial J}{\partial I} + \mu_2 |\dot{z}_s|, \tag{5}$$

where I is updated in the negative gradient of J with a gain μ_1, and the second term $\mu_2|\dot{z}_s|$ is an additional term that has been introduced to improve the ride comfort without sacrificing the handling performance of the vehicle on purpose. To implement (5), the term $\partial J/\partial I$ is calculated as follows.

$$\frac{\partial J}{\partial I} = 2\ddot{z}_s \frac{\partial \ddot{z}_s}{\partial I}, \tag{6}$$

where $\partial \ddot{z}/\partial I$ is the sensitivity of the vertical acceleration with respect to I (detailed derivations are given in Section 3.2), and the term $|\dot{z}_s|$ is estimated using (1) as follows.

$$\ddot{z}_s = -\frac{1}{m_s}\{k_s(z_s - z_u) + f_{mr}(\dot{z}_s - \dot{z}_u, I)\}. \tag{7}$$

Again, $\dot{z}_s$ can be calculated by integrating (7).

3.2 Sensitivity Calculation

The differentiation of (1) with respect to I yields.

$$m_s \frac{d\ddot{z}_s}{dI} + k_s \frac{d(z_s - z_u)}{dI} + \frac{d}{dI} f_{mr}(\dot{z}_s - \dot{z}_u, I) = 0. \tag{8}$$

The last term in (8) can be split into two parts as follows.

$$\frac{d}{dI} f_{mr}(\dot{z}_s - \dot{z}_u, I) = \frac{\partial f_{mr}}{\partial(\dot{z}_s - \dot{z}_u)} \frac{d(\dot{z}_s - \dot{z}_u)}{dI} + \frac{\partial f_{mr}}{\partial I} \tag{9}$$

Using (3), $\partial f_{mr}/\partial(\dot{z}_s - \dot{z}_u)$ and $\partial f_{mr}/\partial I$ can be written as follows.

$$\frac{\partial f_{mr}}{\partial(\dot{z}_s - \dot{z}_u)} = \sum_{k=1}^{6} k(a_k^\circ + b_k^\circ I)(\dot{z}_s - \dot{z}_u)^{k-1}, \tag{10}$$

$$\frac{\partial f_{mr}}{\partial I} = \sum_{k=0}^{6} b_k^\circ (\dot{z}_s - \dot{z}_u)^k. \tag{11}$$

Since the tire spring coefficient is ten times larger than that of the spring stiffness coefficient, and the unsprung-mass m_u is one-tenth of the sprung-mass m_s, the displacement and velocity of the unsprung-mass are not much affected by the current input I. Hence, $d(\dot{z}_s - \dot{z}_u)/dI$ and $d(z_s - z_u)/dI$ can be computed as follows.

$$\frac{d(\dot{z}_s - \dot{z}_u)}{dI} = \frac{d\dot{z}_s}{dI}, \tag{12}$$

$$\frac{d(z_s - z_u)}{dI} = \frac{dz_s}{dI}. \tag{13}$$

Using (9)-(13), (8) can be written as follows.

$$m_s \ddot{s} + \left\{\sum_{k=0}^{6} k(a_k^\circ + b_k^\circ I)(\dot{z}_s - \dot{z}_u)^{k-1}\right\}\dot{s} + k_s s + \sum_{k=0}^{6} b_k^\circ I(\dot{z}_s - \dot{z}_u)^k = 0, \tag{14}$$

where $\ddot{s}$, $\dot{s}$ and s correspond to $d\ddot{z}_s/dI$, $d\dot{z}_s/dI$, and dz_s/dI, respectively. Therefore, the sensitivity $\ddot{s}$ appears as a second-order

differential equation, and by solving (14), dJ/dI in (6) is obtained. Finally, the control law (5) is given as follows.

$$\dot{I} = \mu_1 \frac{2}{m_s}\left\{k_s(z_s - z_u) + \sum_{k=0}^{6}(a_k^{\circ} + b_k^{\circ} I)(\dot{z}_s - \dot{z}_u)^k\right\}\ddot{s} + \mu_2 |\dot{z}_s| \quad (15)$$

3.3 Effect of $\mu_2|\dot{z}_s|$

As discussed earlier, the second term $\mu_2|\dot{z}_s|$ in (5) has been added in order to improve the ride comfort without sacrificing the handling performance of the vehicle. In the case of a passive damper, where $F_{damper} = c_s(\dot{z}_s - \dot{z}_u)$, the resonant peaks are attenuated as the damping coefficient c_s increased; however, the isolations are lost both at high frequency and at frequencies range between the two natural frequencies (see Fig. 6). Therefore, it is desirable to have a large damping coefficient at the resonant frequency and to have a small damping coefficient in the frequency range above the resonant frequency. Fig. 7 depicts the frequency response of the sprung-mass velocity of a typical passive damper. As shown, the maximum magnitude of the sprung-mass velocity appears at the resonant frequency of the sprung-mass. Henceforth, by adding the term $\mu_2|\dot{z}_s|$ in (5), the increase of the damping coefficient at the resonant frequency can be obtained.

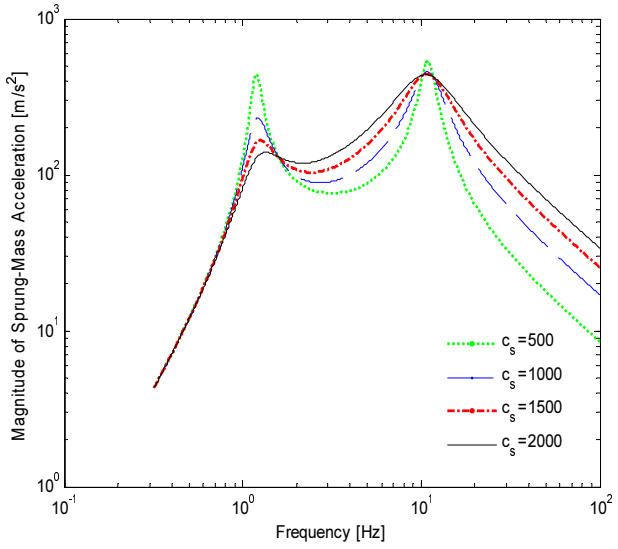

Fig. 6 Frequency responses of the sprung-mass acceleration for three different damping coefficients (simulation results with the values in Table 1)

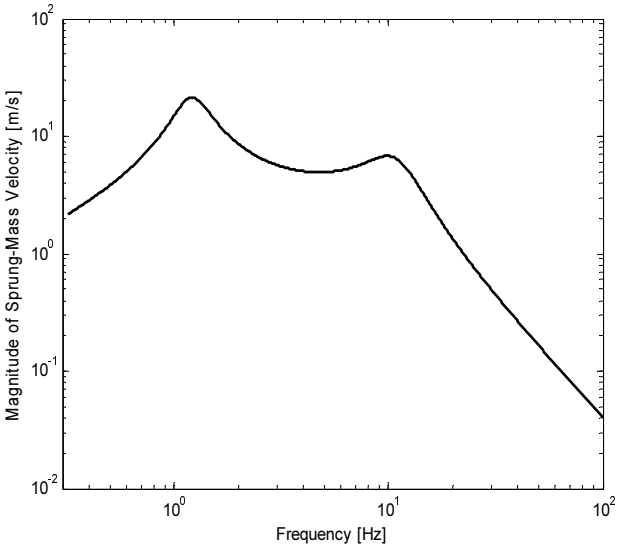

Fig. 7 Frequency response of the sprung-mass velocity in the passive case of Fig. 6

4. Stability Analysis

In this section, the stability of the proposed control law in (15) is analyzed. The following state variables and state vector are defined.

$$\begin{aligned} &x_1 = z_s - z_u, \quad x_2 = \dot{z}_s, \quad x_3 = z_u - z_r, \quad x_4 = \dot{z}_u, \\ &x_5 = I, \quad x_6 = s, \quad \text{and} \quad x_7 = \dot{s}, \end{aligned} \quad (16)$$

$$X = [x_1 \quad x_2 \quad x_3 \ldots x_7]^T. \quad (17)$$

Using (16), the state equations including (1), (2), (3), (6) and (15) are given as follows.

$$\dot{x}_1 = \dot{z}_s - \dot{z}_u = x_2 - x_4 \equiv f_1(X,t), \quad (18)$$

$$\dot{x}_2 = \ddot{z}_s = -\frac{1}{m_s}\left\{k_s x_1 + \sum_{k=0}^{6}(a_k^{\circ} + b_k^{\circ} x_5)(x_2 - x_4)^k\right\} \equiv f_2(X,t), \quad (19)$$

$$\dot{x}_3 = \dot{z}_u - \dot{z}_r = x_4 \equiv f_3(X,t), \quad (20)$$

since $z_r = 0$ can be assumed for stability analysis,

$$\dot{x}_4 = \ddot{z}_u = -\frac{1}{m_u}\left\{-k_s x_1 + k_u x_3 - \sum_{k=0}^{6}(a_k^{\circ} + b_k^{\circ} x_5)(x_2 - x_4)^k\right\} \equiv f_4(X,t), \quad (21)$$

$$\begin{aligned} \dot{x}_5 = \dot{I} &= \mu_1 \frac{2}{m_s}\left\{k_s x_1 + \sum_{k=0}^{6}(a_k^{\circ} + b_k^{\circ} x_5)(x_2 - x_4)^k\right\} \\ &.f_7(X,t) + \mu_2 |x_2| \equiv f_5(X,t), \end{aligned} \quad (22)$$

$$\dot{x}_6 = \dot{s} = x_7 \equiv f_6(X,t), \quad (23)$$

$$\begin{aligned} \dot{x}_7 = \ddot{s} = -\frac{1}{m_s}\Bigg\{ & x_7 \sum_{k=0}^{6}\left(a_k^0 + b_k^0 x_5\right)k\left(x_2 - x_4\right)^{k-1} \\ & + k_s x_6 + \sum_{k=0}^{6} b_k^0 \left(x_2 - x_4\right)^k \Bigg\} \\ \equiv f_7\left(X,t\right). & \end{aligned} \quad (24)$$

By solving the equations (18)-(24), the equilibrium points X_e can be obtained.

$$\begin{aligned} &x_1 = -\frac{a_0^{\circ} + b_0^{\circ} \; x_5}{k_s}, \\ &x_2 = x_3 = x_4 = x_7 = 0, \\ &x_5 = \text{any value}, \\ &x_6 = -\frac{b_0^{\circ}}{k_s}. \end{aligned} \quad (25)$$

Recall that x_5 denotes the current input in the range of [0, 3] A. Now, the linearization of equations (18)-(24) with respect to the equilibrium point $X_e = [-(a_0^\circ + b_0^\circ x_5)/k_s, 0, 0, 0, x_5, -b_0^\circ/k_s, 0]^T$ yields.

$$\dot{X} = \left.\frac{\partial F}{\partial X}\right|_{X_e} X, \tag{26}$$

where

$$\left.\frac{\partial F}{\partial X}\right|_{X_e} = \begin{bmatrix} 0 & 1 & 0 & -1 & 0 & 0 & 0 \\ -\frac{k_s}{m_s} & -\frac{a_1^\circ + b_1^\circ x_5}{m_s} & 0 & \frac{a_1^\circ + b_1^\circ x_5}{m_s} & -\frac{b_0^\circ}{m_s} & 0 & 0 \\ 0 & 0 & 0 & 1 & 0 & 0 & 0 \\ \frac{k_s}{m_u} & \frac{a_1^\circ + b_1^\circ x_5}{m_u} & -\frac{k_u}{m_u} & -\frac{a_1^\circ + b_1^\circ x_5}{m_u} & \frac{b_0^\circ}{m_u} & 0 & 0 \\ 0 & \mu_2 & 0 & 0 & 0 & 0 & 0 \\ 0 & 0 & 0 & 0 & 0 & 0 & 1 \\ 0 & -\frac{b_1}{m_s} & 0 & \frac{b_1}{m_s} & 0 & -\frac{k_s}{m_s} & -\frac{a_1^\circ + b_1^\circ x_5}{m_s} \end{bmatrix} \tag{27}$$

Observing the first, third, and fifth rows in (27), the existence of a linear dependence relationship among them can be seen. Hence, $\partial F/\partial X|_{X_e}$ has nullity 1 and any value in the nullspace can be an equilibrium point. Also, since $\partial F/\partial X|_{X_e}$ involves x_5, the eigenvalues of $\partial F/\partial X|_{X_e}$ is given as a function of x_5. Over the range of x_5 (the current input 0~3 A), the real parts of all the eigenvalues are negative except one (see Fig. 8 of reference 11). Therefore, the local stability is proven.

5. Simulations

Simulation is performed for three aspects, which are the role of the second term in (5), the performance of the sensitivity control law in comparison with the skyhook control, and the robustness of the proposed control algorithm against the variations of the sprung-mass and spring stiffness coefficient.

5.1 The effect of $\mu_2|\dot{z}_s|$

Fig. 8 compares the sprung-mass acceleration of the sensitivity algorithm for $\mu_1 = 0.5$ and $\mu_2 = 0$ with that of a passive damper. As shown in Fig. 8, the sensitivity control shows poor performance in the lower frequency range. However, as shown in Fig. 9, by increasing μ_2 values, improved performances in the lower frequency range as well as in the high frequency range can be obtained. It is desirable to have a large μ_2-value below 3 Hz and to have a small μ_2-value above 3 Hz.

5.2 Comparison with the Skyhook Control

The skyhook control algorithm is given as follows.[32]

$$\begin{aligned} &f_{mr} = c_{sky}\dot{z}_s, \quad \text{if} \quad \dot{z}_s(\dot{z}_s - \dot{z}_u) > 0, \quad c_{sky} = 1{,}500, \\ &f_{mr} = 0, \quad \text{if} \quad \dot{z}_s(\dot{z}_s - \dot{z}_u) < 0. \end{aligned} \tag{28}$$

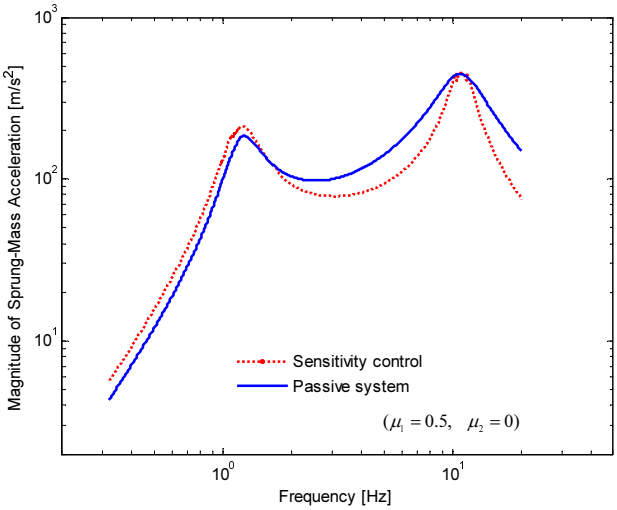

Fig. 8 Frequency responses of the sprung-mass acceleration with μ_1=0.5 and μ_2=0

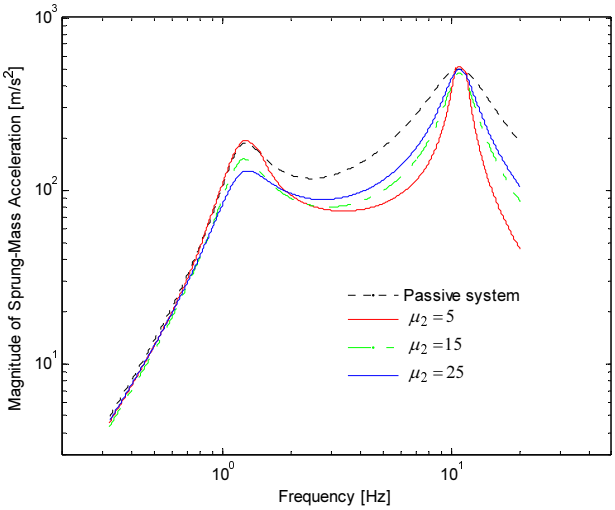

Fig. 9 Frequency responses of the sprung-mass acceleration for various values of μ_2 (μ_1=0.5)

Fig. 10 compares the passive damper, the skyhook control law with $c_{sky} = 1{,}500$, and the sensitivity control law for $\mu_1 = 0.5$ and $\mu_2 = 25$. At the resonant frequency, both the skyhook control and the sensitivity control show the similar performance, but at the resonant frequency of the unsprung-mass of 11.7 Hz, the sensitivity control shows better performance than the skyhook control. Notice that skyhook control focuses on the sprung-mass in which, as the value of c_{sky} increases, the motion of sprung-mass decreases but the motion of the unsprung-mass increases.

5.3 Robustness

$\ddot{s}$ in (14) is calculated with the sprung-mass ($m_s = 390$ kg) and the spring stiffness coefficient ($k_s = 25{,}000$ N/m). Therefore, deterioration of the control performance may be expected if there is some discrepancy between the used values and real values. To check for deterioration, the sprung-mass was increased from 390 kg to 450 kg and the spring stiffness coefficient was decreased from 25,000 N/m to 22,000 N/m. Figs. 11 and 12 depict the

transmissibility of the sprung-mass displacement from the road displacement. Figs. 13 and 14 compare the frequency responses of the sprung-mass acceleration in the presence of uncertainties.

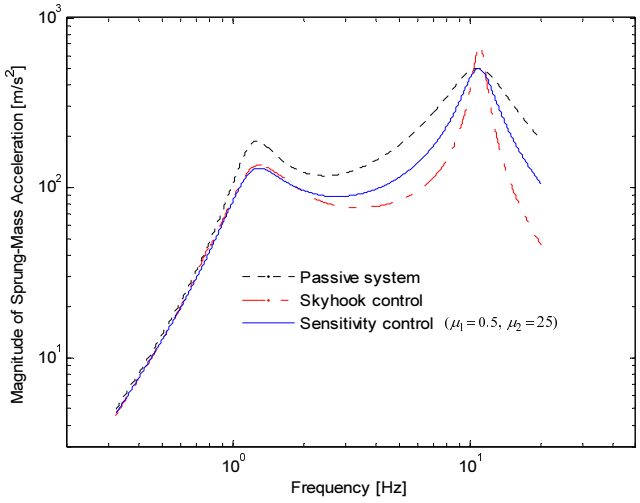

Fig. 10 Comparison of the frequency responses of the sprung-mass acceleration

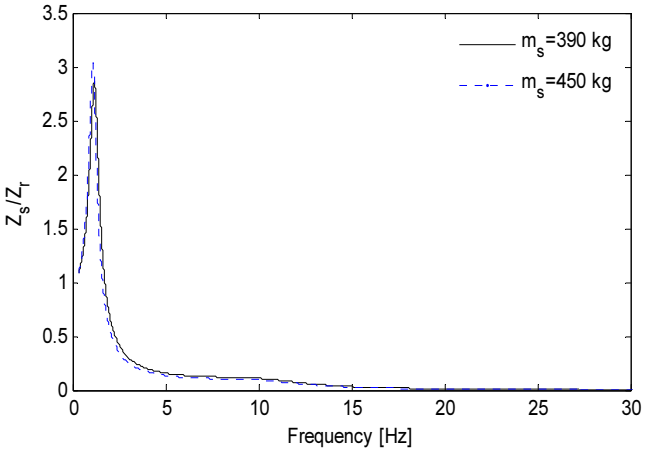

Fig. 11 Transmissibility comparison between two sprung masses

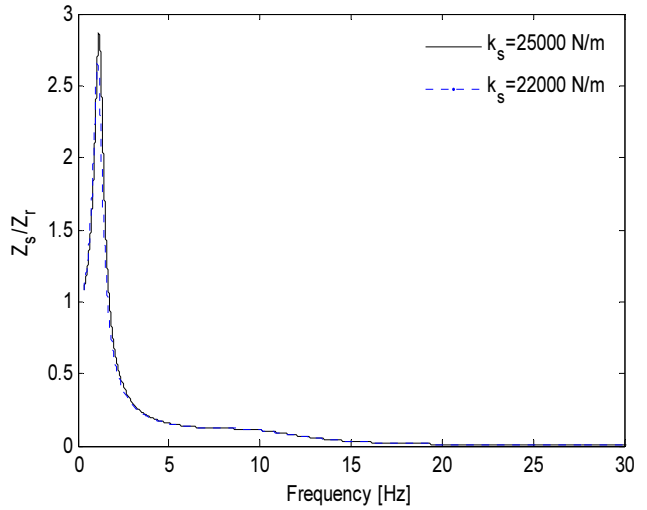

Fig. 12 Transmissibility comparison between two spring stiffness coefficient

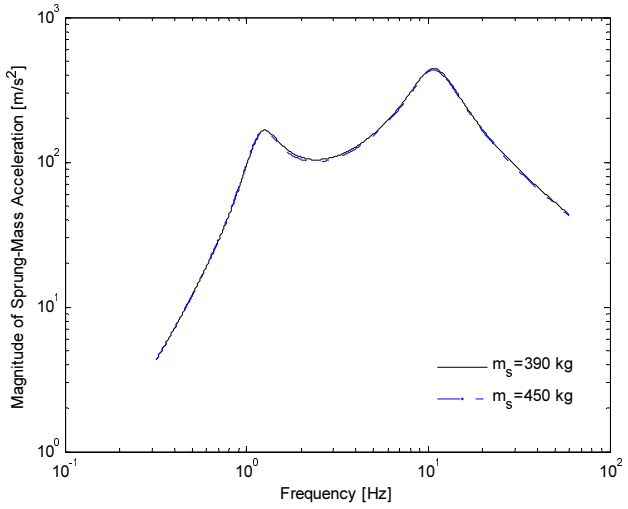

Fig. 13 Comparison of the frequency responses of the sprung-mass

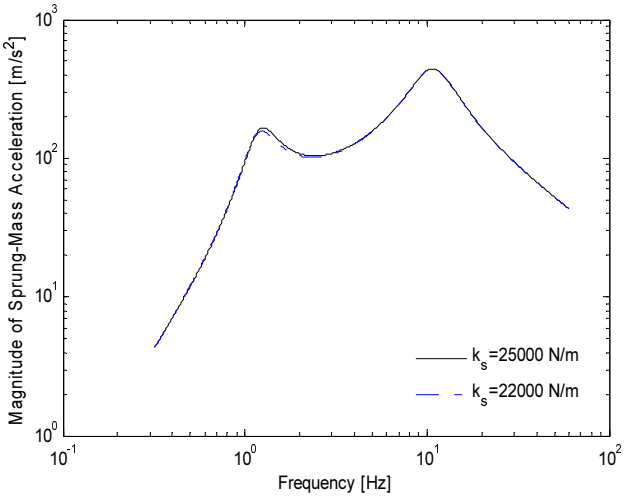

Fig. 14 Comparison of the frequency responses of the sprung-mass

6. Conclusions

In this paper, a sensitivity control law combining the negative gradient of the performance index and the weighted absolute velocity of the sprung-mass is developed to improve the ride quality without sacrificing the handling performance. The proposed algorithm demonstrated similar performance with the passive damper at the resonant frequency of the unsprung-mass, but an improved performance of the ride quality at the resonant frequency of the sprung-mass. It was desirable to have a large value of μ_2 for a low frequency road input, but to have a small value for a high frequency road input.

ACKNOWLEDGMENT

This work was supported by the Regional Research Universities Program (Research Center for Logistics Information Technology, LIT) granted by the Ministry of Education, Science and Technology, Korea.

REFERENCES

1. Choi, S. B., Park, D. W. and Park, Y. P., "A Hysteresis Model for the Field-Dependent Damping Force of a Magnet-orheological Damper," Journal of Sound and Vibration, Vol. 245, No. 2, pp. 375-383, 2001.
2. Lee, S. K. and Choi, S. B., "Hysteresis Model of Damping Force of MR Damper for a Passenger Car," Journal of the Korean Society Automotive Engineers, Vol. 9, No. 1, pp. 189-197, 2001.
3. Liu, Y. Q., Matsuhisa, H., Utsuno, H. and Park, J. G., "Variable Damping and Stiffness Vibration Control with Magnetorheological Fluid Dampers for Two Degree-of-Freedom System," JSME International Journal, Series C, Vol. 49, No. 1, pp. 156-162, 2006.
4. Song, X. Ahmadian, M. Southward, S. and Miller, L. R., "An Adaptive Semiactive Control Algorithm for Magnet-orheological Suspension Systems," ASME Journal Vibration Acoustics, Vol. 127, No. 5, pp. 493-502, 2005.
5. Ahmadian, M. and Christopher, A. P., "A Quarter-Car Experimental Analysis of Alternative Semi-Active Control Methods," Journal of Intelligent Material Systems and Structures, Vol. 11, No. 8, pp. 604-612, 2000.
6. Ahn, K. K., Truong, D. Q. and Islam, M. A., "Modeling of a Magneto-Rheological (MR) Fluid Damper Using a Self Tuning Fuzzy Mechanism," Journal of Mechanical Science and Technology, Vol. 23, No. 5, pp. 1485-1499, 2009.
7. Goncalves, F. D. and Ahmadian, M., "A Hybrid Control Policy for Semi-Active Vehicle Suspensions," Shock and Vibration, Vol. 10, No. 1, pp. 59-69, 2003.
8. Park, C., Kim, Y. and Bae, D., "Sensitivity Analysis of Suspension Characteristics for Korean High Speed Train," Journal of Mechanical Science and Technology, Vol. 23, No. 4, pp. 938-941, 2009.
9. Jang, K.-I., Seok, J., Min, B. K. and Lee, S. J., "A 3D Model for Magnetorheological Fluid that Considers Neighboring Particle Interactions in 2D Skewed Magnetic Fields," Int. J. Precis. Eng. Manuf., Vol. 10, No. 1, pp. 115-118, 2009.
10. Afshari, H. H., Ehramianpour, M. and Mohammadi, M., "Investigation of a Nonlinear Dynamic Hydraulic System Model Through the Energy Analysis Approach," Journal of Mechanical Science and Technology, Vol. 23, No. 11, pp. 2973-2979, 2009.
11. Kim, T. S., Hong, K. S., Kim, R. K., Park, J. W. and Huh, C. D., "Modified Sensitivity Control of a Semi-Active Suspension System with MR-Damper for Ride Comfort Improvement," Korean Society of Mechanical Engineers, Vol. 31, No. 1, pp. 129-138, 2007.
12. Yi, K. S. and Hedrick, J. K., "Observer-Based Identification of Nonlinear System Parameters," ASME Transactions, Journal of Dynamic Systems, Measurement, and Control, Vol. 117, No. 2, pp. 175-182, 1995.
13. Lin, J. S. and Kanellakopoulos, I., "Nonlinear Design of Active Suspensions," IEEE Control System Magazine, Vol. 17, No. 3, pp. 45-59, 1997.
14. Lee, U., "A Proposition for New Vehicle Dynamic Performance Index," Journal of Mechanical Science and Technology, Vol. 23, No. 4, pp. 889-893, 2009.
15. Lee, S.-H., Park, T.-W., Park, J.-K., Yoon, J.-W., Jun, K.-J. and Jung, S.-P., "A Fatigue Life Analysis of Wheels on Guideway Vehicle Using Multibody Dynamics," Int. J. Precis. Eng. Manuf., Vol. 10, No. 5, pp. 79-84, 2009.
16. Yi, K. S. and Song, B. S., "Observer Design for Semi-Active Suspension Control," Vehicle System Dynamics, Vol. 32, No. 2-3, pp. 129-148, 1999.
17. Glauser, G. L., Juang, J. N. and Sulla, J. L., "Optimal Active Vibration Absorber: Design and Experimental Results," ASME Transactions, Journal of Vibration and Acoustics, Vol. 117, No. 4, pp. 165-171, 1995.
18. Jeon, J.-Y., "Passive Vibration Damping Enhancement of Piezoelectric Shunt Damping System Using Optimization Approach," Journal of Mechanical Science and Technology, Vol. 23, No. 5, pp. 1435-1445, 2009.
19. Heo, S.-J., Park, K. and Son, S.-H., "Modeling of Continuously Variable Damper for Design of Semi-Active Suspension Systems," International Journal of Vehicle Design, Vol. 31, No. 1, pp. 41-57, 2003.
20. Ahn, H.-J., "Performance Limit of a Passive Vertical Isolator Using a Negative Stiffness Mechanism," Journal of Mechanical Science and Technology, Vol. 22, No. 12, pp. 2357-2364, 2008.
21. Hong, K. S., Jeon, D. S., Yoo, W. S., Sunwoo, H., Shin, S. Y., Kim, C. M. and Park, B. S., "A New Model and an Optimal Pole-Placement Control for the Macpherson Suspension System," SAE Paper, No. 1999-01-1331, pp. 267-276, 1999.
22. Ambrósio, J. and Verissimo, P., "Sensitivity of a Vehicle Ride to the Suspension Bushing Characteristics," Journal of Mechanical Science and Technology, Vol. 23, No. 4, pp. 1075-1082, 2009.
23. Liu, Y., Waters, T. P. and Brennan, M. J., "A Comparison of Semi-Active Damping Control Strategies for Vibration Isolation of Harmonic Disturbances," Journal of Sound and Vibration, Vol. 280, No. 1, pp. 21-39, 2005.
24. Kim, B. S., Spiryagin, M., Kim, B. S. and Yoo, H. H., "Analysis of the Effects of Main Design Parameters Variation on the Vibration Characteristics of a Vehicle Sub-frame," Journal of Mechanical Science and Technology, Vol. 23, No. 4, pp. 960-963, 2009.

25. Roh, H. S. and Park, Y., "Stochastic Optimal Preview Control of an Active Vehicle Suspension," Journal of Sound and Vibration, Vol. 220, No. 2, pp. 313-330, 1990.

26. Park, J.-H. and Rhim, S., "Experiments of Optimal Delay Extraction Algorithm Using Adaptive Time-Delay Filter for Improved Vibration Suppression," Journal of Mechanical Science and Technology, Vol. 23, No. 4, pp. 997-1000, 2009.

27. So, S.-G. and Karnopp, D., "Active Dual Mode Tilt Control for Narrow Ground Vehicle," International Journal of Vehicle System Dynamics, Vol. 27, No. 1, pp. 19-36, 1997.

28. Kim, H. and Yoon, Y. S., "Semi-Active Suspension with Preview Using a Frequency-Shaped Performance Index," Vehicle System Dynamics, Vol. 24, No. 10, pp. 759-780, 1995.

29. Kim, I. and Kim, Y.-S., "Active Vibration Control of Trim Panel Using a Hybrid Controller to Regulate Sound Transmission," Int. J. Precis. Eng. Manuf., Vol. 10, No. 1, pp. 41-47, 2009.

30. Lee, S.-H., Park, T.-W., Moon, K.-H., Choi, S.-H. and Jun, K.-J., "The Articulated Vehicle Dynamic Analysis Using the AWS (All Wheel Steering) ECU (Electronic Control Unit) Test," Journal of Mechanical Science and Technology, Vol. 23, No. 4, pp. 923-926, 2009.

31. Lee, H., Park, K., Hwang, T., Noh, K., Heo, S.-J., Jeong, J. I., Choi, S., Kwak, B. and Kim, S., "Development of Enhanced ESP System Through Vehicle Parameter Estimation," Journal of Mechanical Science and Technology, Vol. 23, No. 4, pp. 1046-1049, 2009.

32. Alleyne, A. and Hedrick, J. K., "Nonlinear Adaptive Control of Active Suspensions," IEEE Transaction on Control Systems Technology, Vol. 3, No. 1, pp. 94-101, 1995.

33. Park, Y. and Jung, B., "Development of Damper for New Electronically Controlled Power-Steering System by Magneto-Rheorogical Fluid: MRSTEER," International Journal of Vehicle Design, Vol. 33, No. 1-3, pp. 103-114, 2003.

34. Jun, K.-J., Park, T.-W. and Jung, S.-P., "Optimization of the Industrial Guide-way Vehicle to Improve the Running Stability," Journal of Mechanical Science and Technology, Vol. 23, No. 4, pp. 1098-1101, 2009.

35. Yoo, W. S., Park, D. W., Kim, M. S. and Hong, K. S., "Optimum Air Pressure for an Air-Cell Seat to Enhance Ride Comfort," International Journal of Automotive Technology, Vol. 6, No. 3, pp. 251-257, 2005.

36. Lee, Y. and Jeon, D. Y., "A Study on the Vibration Attenuation of a Driver Seat Using an MR Fluid Damper," Journal of Intelligent Material Systems and Structures, Vol. 13, No. 7-8, pp. 437-441, 2002.

37. Jung, J.-K., Youm, W.-S. and Park, K.-H., "Vibration Reduction Control of a Voice Coil Motor (VCM) Nano Scanner," Int. J. Precis. Eng. Manuf., Vol. 10, No. 3, pp. 167-170, 2009.

38. Kong, Y.-M., Choi, S.-H., Song, J.-D, Yang, B.-S. and Choi, B. K., "Application of Nonlinear Integer Programming for Vibration Reduction Optimum Design of Ship Structure," Journal of Mechanical Science and Technology, Vol. 23, No. 8, pp. 2085-2096, 2009.

39. Park, C. and Jeon, D. Y., "Semiactive Vibration Control of a Smart Seat with an MR Fluid Damper Considering its Time Delay," Journal of Intelligent Material Systems and Structures, Vol. 13, No. 7-8, pp. 521-524, 2002.

40. Choi, S. B., Park, D. W. and Suh, M. S., "Fuzzy Sky-Ground Hook Control of a Tracked Vehicle Featuring Semi-Active Electrorheological Suspension Units," ASME Trans., Journal of Dynamic Systems, Measurement, and Control, Vol. 124, No. 1, pp. 150-157, 2002.

41. Jang, T. S., Kwon, S. H. and Han, S. L., "A Novel Method for Non-parametric Identification of Nonlinear Restoring Forces in Nonlinear Vibrations from Noisy Response Data: A Conservative System," Journal of Mechanical Science and Technology, Vol. 23, No. 11, pp. 2938-2947, 2009.

42. Du, H., Sze, K. Y. and Lam, J., "Semi-active H_Infinity Control of Vehicle Suspension with Magnetorheological Dampers," Journal of Sound and Vibration, Vol. 283, No. 3, pp. 981-996, 2005.

43. Cho, J. M., Hur, N. and Joh, J. S., "Control of Rotary MR Damper Suspension System," Proceedings of Korea Society of Precision Engineering Spring Conference, pp. 43-44, 2007.

44. Sohn, H. C., Hong, K. T., Hong, K. S. and Yoo, W. S., "An Adaptive LQG Control of Semi-Active Suspension Systems," International Journal of Vehicle Design, Vol. 34, No. 4, pp. 309-326, 2004.

45. Azadi, S., Azadi, M. and Zahedi, F., "NVH Analysis and Improvement of a Vehicle Body Structure Using DOE Method," Journal of Mechanical Science and Technology, Vol. 23, No. 11, pp. 2980-2989, 2009.

46. Karnopp, D. C., Crosby, M. J. and Harwood, R. A. "Vibration Control Using Semi-Active Force Generator," ASME Journal of Engineering for Industry, Vol. 96, No. 2, pp. 619-626, 1974.

47. Park, S.-S., Kim, J., Choi, Y. and Chang, J.-H., "Effect of Mechanical Damping and electrical Conductivity on the Dynamic Performance of a Novel Electromagnetic Engine Valve Actuator," Int. J. Precis. Eng. Manuf., Vol. 9, No. 3, pp. 72-74, 2008.

48. Hong, K. S., Sohn, H. C. and Hedrick, J. K., "Modified Skyhook Control of Semi-Active Suspensions: a New Model, Gain Scheduling, and Hardware-in-the-Loop Tuning," ASME Trans., Journal of Dynamic Systems, Measurement, and Control, Vol. 124, No. 1, pp. 158-167, 2002.

49. Besinger, F. H., Cebon, D. and Cole, D. J., "Force Control of a

Semi-Active Damper," Vehicle System Dynamics, Vol. 24, No. 9, pp. 695-723, 1995.

50. Novak, M. and Valasek, M., "A New Concept of Semi-Active Control of Trucks Suspension," Proc. of AVEC 96, International Symposium on Advanced Vehicle Control, Aachen University of Technology, pp. 141-151, 1996.

51. Sohn, J.-H., Lee, S.-K. and Yoo, W.-S., "Hybrid Neural Network Bushing Model for Vehicle Dynamics Simulation," Journal of Mechanical Science and Technology, Vol. 22, No. 12, pp. 2365-2374, 2008.

52. Jung, J.-K., Youm, W.-S. and Park, K.-H., "Vibration Reduction Control of a Voice Coil Motor (VCM) Nano Scanner," Int. J. Precis. Eng. Manuf., Vol. 10, No. 3, pp. 167-170, 2009.

53. Bingham, E. C., "Fluidity and Plasticity," McGraw-Hill, 1992.

54. Bouc, R., "Force Vibration of Mechanical Systems with Hysteresis," 4th Conf. on Nonlinear Oscillation, 1967.

55. Wen, Y. K., "Approximate Method for Non-Linear Random Vibration," Journal of the Engineering Mechanics Division, Vol. 101, No. 4, pp. 389-401, 1975.

56. Yang, I., Park, M. S. and Chu, C. N., "Micro ECM with Ultrasonic Vibrations Using a Semi-cylindrical Tool," Int. J. Precis. Eng. Manuf., Vol. 10, No. 2, pp. 5-10, 2009.